

Communication

# Iridescence and Luminescence from Opal Matrices for Show Business

Nikolai V. Gaponenko <sup>1,\*</sup>, Svetlana M. Kleshcheva <sup>2</sup>, Ekaterina I. Lashkovskaya <sup>1</sup>, Uladzimir A. Zaitsau <sup>1</sup>, Vladimir A. Labunov <sup>1</sup>, Bashar Z. S. Hamadneh <sup>1</sup>, Vadim D. Zhivulko <sup>3</sup>, Alexander V. Mudryi <sup>3</sup>, Yuriy V. Radyush <sup>3</sup>, Nikolai I. Kargin <sup>4</sup> and Tamara F. Raichenok <sup>5</sup>

<sup>1</sup> Laboratory of Nanophotonics, Belarusian State University of Informatics and Radioelectronics, 220013 Minsk, Belarus; e.lashkovskaia@bsuir.by (E.I.L.); uladzimir.a.zaitsau@gmail.com (U.A.Z.); labunov@bsuir.by (V.A.L.); bhamadneh@yahoo.com (B.Z.S.H.)

<sup>2</sup> Independent Researcher, 121354 Moscow, Russia; svetlanaklecheva@yandex.ru

<sup>3</sup> Scientific-Practical Materials Research Centre, National Academy of Sciences of Belarus, 220072 Minsk, Belarus; zhivulko@physics.by (V.D.Z.); mudryi@physics.by (A.V.M.); radyush@physics.by (Y.V.R.)

<sup>4</sup> National Research Nuclear University “MEPhI”, 115409 Moscow, Russia; nikargin@mephi.ru

<sup>5</sup> Stepanov Institute of Physics, National Academy of Sciences of Belarus, 220072 Minsk, Belarus; raitf@ifanbel.bas-net.by

\* Correspondence: gaponenko@bsuir.by; Tel.: +375-17-293-8875

## Abstract

The paper reports on obtaining visually appealing images from opal matrices to artificial samples comprising regular packing of monodisperse silica globules. We show the images of iridescence, photoluminescence, and both of them simultaneously, exciting upconversion luminescence of  $\text{Er}^{3+}$  ions from  $\text{BaTiO}_3$  xerogel/opal matrix. Opal matrix with  $\text{BaTiO}_3$  xerogel doped with  $\text{Er}^{3+}$  and  $\text{Yb}^{3+}$  ions demonstrates upconversion luminescence under excitation with the wavelength 980 nm of the laser with the main bands ranging from 500 to 570 nm and 640–700 nm, corresponding to the transitions from the excited states  $^2\text{H}_{11/2}$ ,  $^4\text{S}_{3/2}$ ,  $^4\text{F}_{9/2}$ ,  $^4\text{I}_{9/2}$  to the ground state  $^4\text{I}_{15/2}$  of trivalent Er ions. In our view, the synthesis of opal matrices along with the generation of luminescent xerogels doped, for example, with trivalent lanthanides, is a promising approach for obtaining colorful images, always very individual and often very attractive, bringing joy and pleasure at concerts and other show business events.



Received: 17 July 2025

Revised: 3 September 2025

Accepted: 6 September 2025

Published: 10 September 2025

**Citation:** Gaponenko, N.V.; Kleshcheva, S.M.; Lashkovskaya, E.I.; Zaitsau, U.A.; Labunov, V.A.; Hamadneh, B.Z.S.; Zhivulko, V.D.; Mudryi, A.V.; Radyush, Y.V.; Kargin, N.I.; et al. Iridescence and Luminescence from Opal Matrices for Show Business. *Photonics* **2025**, *12*, 908. <https://doi.org/10.3390/photonics12090908>

**Copyright:** © 2025 by the authors. Licensee MDPI, Basel, Switzerland. This article is an open access article distributed under the terms and conditions of the Creative Commons Attribution (CC BY) license (<https://creativecommons.org/licenses/by/4.0/>).

## 1. Introduction

As was reported in 1968 by Sanders, “in gem quality opal the particles are remarkably uniform in size, and they were therefore able to pack together regularly to form a pseudo-crystal” [1]. The effect of iridescence of artificial opals is explained by the photonic band gap effect of 3D photonic crystals [2,3]. Photonic band gap is shifted for the opals impregnated with liquids or after synthesis of solids like xerogels in space between the globules [3–5]. Photonic band gap materials like opals or inverted opals influence spontaneous emission from the excited states of the embedded species [6,7].

Opal matrices are an intermediate product of opal synthesis; they are more porous and more fragile and about ten times cheaper compared to natural jewelry opals. Unlike natural or synthetic gem opals, opal matrices may not exhibit iridescence. However, opal

matrices can exhibit iridescence in liquids, and the color of this type of photonic crystal can change. Recently we proposed to use the images of opal matrices for show and to create the color images using simultaneously the effects of iridescence and luminescence using opal matrices containing light-emitting species inside [8]. In this paper, we begin to describe several experiments that we conducted to create color images using the iridescence and luminescence effects of the opal matrix that contains luminescent xerogels inside. We also demonstrate how the user possessing several opal matrices can manipulate the creation of virtual color images using almost any available improvised experimental tools.

## 2. Materials and Methods

In the experiment 4 opal matrices produced in accordance with the patent [9] were used. These matrices were chosen in order to demonstrate iridescence and change in the color upon liquid impregnation as well as to observe room-temperature up-conversion luminescence after synthesis of Er- and Yb-doped  $\text{BaTiO}_3$  xerogel. Ethanol was used for immersion of the opal matrices in order to reduce diffuse scattering of the media of silica globules and interglobular space of the opal matrices [3]. With the aim of obtaining color images, 4 samples were investigated, designated as samples #1, #2, #3, #4:

1. Opal matrices without xerogel inside (as-grown) immersed in ethanol (samples #1 and #2).
2. Opal matrix immersed once in sol corresponding to Er- and Yb-doped  $\text{BaTiO}_3$  xerogel (BAT-sol) and annealed at 450 °C for 30 min (sample #3) and immersed in ethanol.
3. Opal matrix with  $\text{BaTiO}_3$  xerogel doped with Er and Yb ( $\text{BaTiO}_3:(\text{Er,Yb})$  xerogel) inside and annealed at 600 °C (sample #4). This matrix was immersed in BAT-sol several times, followed by drying and annealing at 450 °C for 30 min after each immersion, then the matrix was finally annealed at 600 °C for 30 min.

To observe upconversion luminescence under excitation by a 980 nm laser line, a sol with an erbium to ytterbium ratio of 1 to 7 was prepared to obtain a  $\text{BaTiO}_3:(\text{Er,Yb})$  xerogel, namely  $\text{Ba}_{0.76}\text{Er}_{0.03}\text{Yb}_{0.21}\text{TiO}_3$ , using the following procedure. Two solutions were prepared. Titanium isopropoxide ( $\text{Ti}(\text{OC}_3\text{H}_7)_4$ ) (97%, Sigma-Aldrich, Steinheim, Germany) was dissolved in acetylacetone ( $\text{CH}_3\text{COCH}_2\text{COCH}_3$ ) (analytical grade, AO Vekton, Saint Petersburg, Russia) and stirred until the solution cooled. Barium acetate ( $\text{Ba}(\text{CH}_3\text{COO})_2$ ) (ACS reagent 99%, Sigma-Aldrich, Steinheim, Germany) was separately dissolved in distilled water and stirred until completely dissolved. Erbium acetate hydrate ( $\text{Er}(\text{CH}_3\text{COO})_3 \cdot x\text{H}_2\text{O}$ ) (99.9% trace metal basis, Sigma-Aldrich, Milwaukee, WI, USA) was added to the barium acetate solution and stirred until completely dissolved. Then, ytterbium acetate hydrate ( $\text{Yb}(\text{CH}_3\text{COO})_3 \cdot x\text{H}_2\text{O}$ ) (99.95% trace metal basis, Sigma-Aldrich, Milwaukee, WI, USA) was added to the barium and erbium acetate solution and stirred until completely dissolved. Acetic acid ( $\text{CH}_3\text{COOH}$ ) was added to the Ba, Er, and Yb acetate solution and stirred for 5 min. Then, solutions of titanium isopropoxide and Ba, Er, and Yb acetates were mixed and stirred for 5 min. Then, ethanol ( $\text{C}_2\text{H}_5\text{OH}$ ) was added to this solution and stirred for 1.5 h. The amount of titanium isopropoxide, barium acetate, and erbium and ytterbium acetate hydrates was selected so that the  $\text{Ti}/(\text{Ba} + \text{Er} + \text{Yb})$  ratio corresponded to the stoichiometric composition of barium titanate in the films (i.e.,  $\text{Ti}:(\text{Ba} + \text{Er} + \text{Yb}) = 1:1$ ).

The reflection spectra were measured on an MS122 spectrophotometer (PROSCAN Special Instruments, Minsk, Belarus).

Experiments with upconversion photoluminescence (PL spectra and images) were carried out under continuous wave (CW) optical excitation. A focused 980 nm laser beam of a 200 mW diode module was used for the excitation of the upconversion PL (power density  $J \sim 10 \text{ W/cm}^2$ ) in the CW mode. The emission in the visible range was focused

on the entrance slit of a 0.6 m grating spectrometer equipped with 1200 gr/mm gratings, and the PL intensity was measured using a R 9110 Hamamatsu photomultiplier tube (Hamamatsu photonics K.K., Hamamatsu City, Japan) that was sensitive in the spectral range of 200–850 nm. The spectral resolution of the PL measurement system was  $\sim 0.6$  nm. A lock-in amplifier with mechanical chopping at a frequency of approximately 20 Hz was used for the signal recovery.

Images of opal matrices were obtained with the use of a microscope camera High Cloud (Shenzhen, China) with a 48-megapixel matrix, 4k ( $3840 \times 2160$ ) frame resolution, and a  $130\times$  lens.

### 3. Results and Discussion

Figures 1–3 show images of opal matrices (samples #1, #2, and #3) obtained using only one white light source—a white LED flashlight from a mobile phone. As the opal matrix is impregnated with ethanol, diffuse scattering decreases and the sample becomes more transparent [3]. The white spot in the center of the sample outlines an area that is not yet impregnated and therefore less transparent. The shape of this unimpregnated area is an individuality of the opal matrix, as is the matrix itself. An example of impregnation with ethanol, illustrating the time scale information, is given for sample #1 by the Supplementary Materials S1, Video S1; the duration of the video is 11 s, and it is in real time. The images from (a) to (e) in Figure 1 were captured within two minutes.

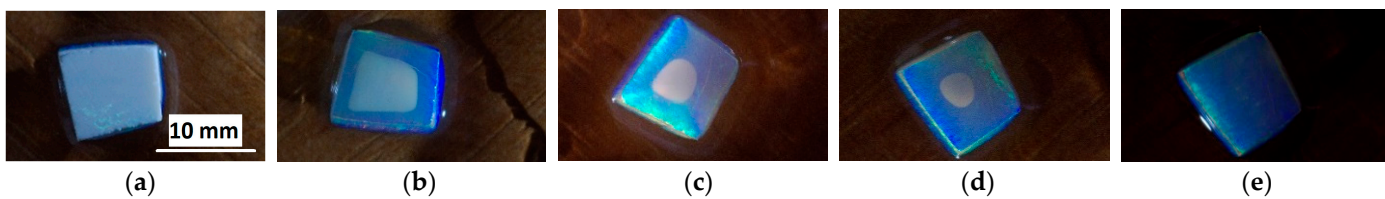


**Figure 1.** Images of opal matrix (sample #1 as-received) immersed in ethanol at different stages of ethanol impregnation. The size of the sample is about  $10 \times 9 \times 4$  mm. The sample was placed on a horizontal surface. From left to right—from initial impregnation to final impregnation. All images are taken from the same sample. The sample was illuminated with a white LED flashlight. The images from (a) to (e) were captured within two minutes.

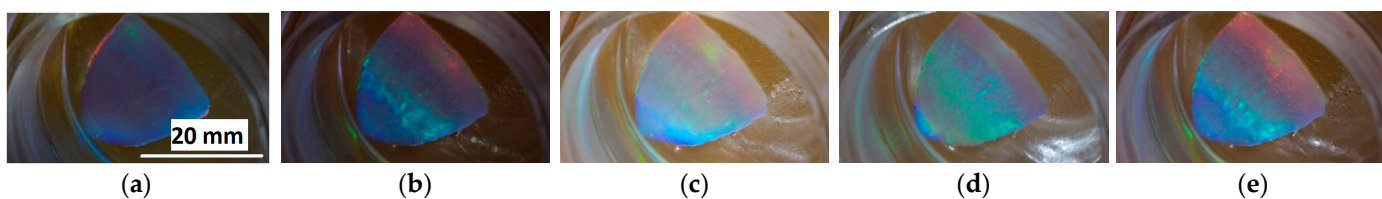


**Figure 2.** Images of opal matrix (sample #2 as-received). The sample resembles the shape of an equilateral triangle with a side of about 19 mm and a thickness of 3 mm. All images are taken from the same sample. The sample was placed in an opened weighing bottle, which was placed on a horizontal surface and was partially filled with ethanol. The sample was illuminated with a white LED flashlight. The images from (a) to (e) differ from each other only because of the change in the angle of illumination and the distance from the light source to the sample manually.

Figure 2 demonstrates sample #2 impregnated with ethanol. This sample is impregnated completely, as is the sample in Figure 1e, unlike the sample shown in Figure 1a–d. The images from (a) to (e) differ from each other only because of the change in the angle of illumination and the distance from the light source to the sample manually. This sample displays a rich range of colors, and again we used only one light source—a white LED flashlight.

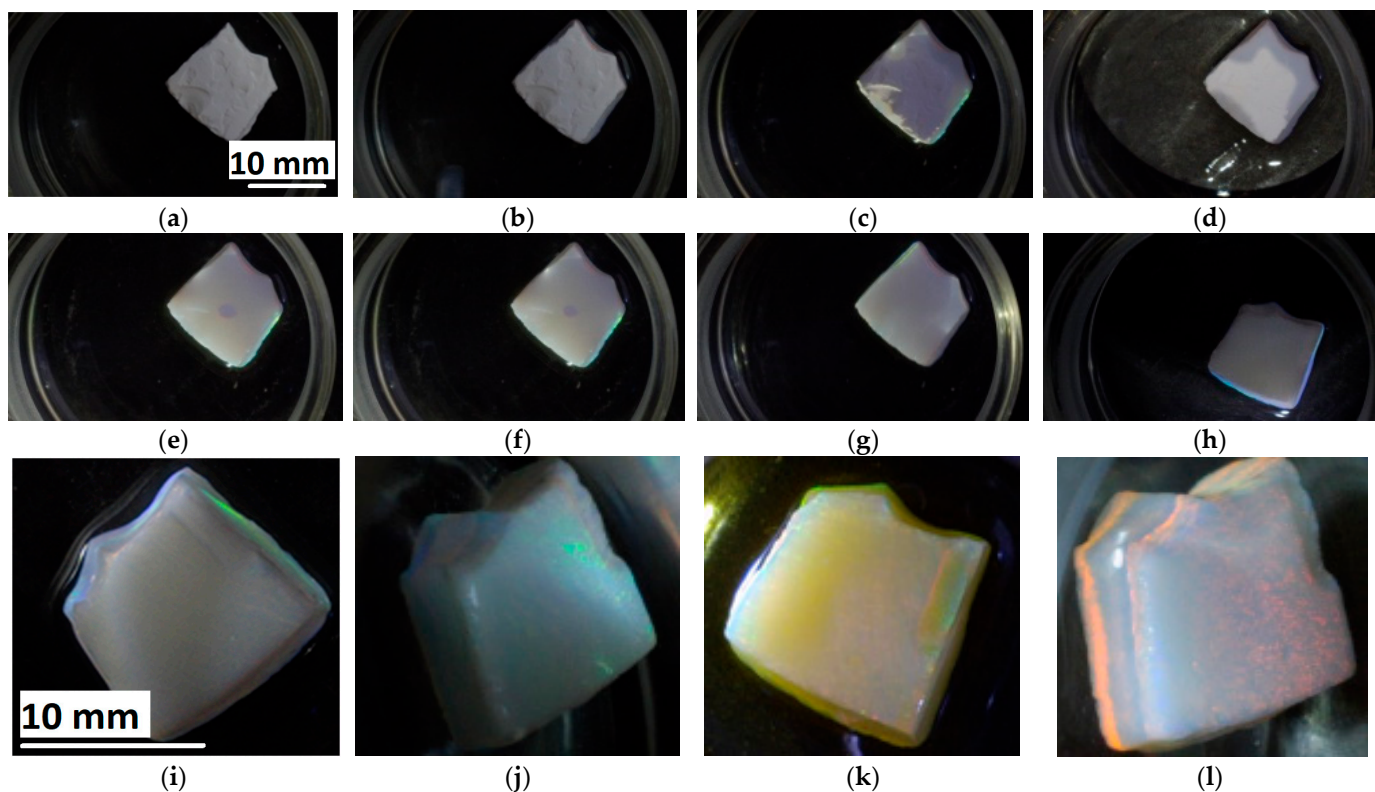


**Figure 3.** Images of opal matrix (sample #3). The size of the sample is about  $12 \times 12 \times 4$  mm. All images are taken within one hour from the same sample, which is impregnating in ethanol. Before impregnation in ethanol, the sample was immersed with BAT-sol, then dried and annealed at  $450^{\circ}\text{C}$  for 30 min. From (a–h)–the sample is located horizontally, (a)–beginning of impregnation, (h)–end of impregnation. From (i–l): the weighing bottle with the sample was turned arbitrarily towards the camera.

Figure 3 also illustrates the stages of impregnation in ethanol for sample #3. As impregnation occurs, the iridescence is coming. After impregnation in ethanol, the sample also demonstrates bright iridescence.

Application of other solvents that reduce diffuse scattering of opals or opal/xerogel structures is also possible; however, it should be noted that the photonic band gap position and color of the opal matrix depend on the refractive index of the solvent [3,5].

This sample #3, which was immersed in BAT-sol and annealed at  $450^{\circ}\text{C}$  for 30 min, does not demonstrate upconversion luminescence. Noteworthy, both of the effects—upconversion luminescence and iridescence—were observed for sample #4 also immersed in BAT-sol followed by annealing at  $600^{\circ}\text{C}$  for 30 min (Figure 4). At higher annealing temperatures or prolonged annealing for several hours, sintering of the xerogel/opal matrix structure can lead to the disappearance of the photonic stop band and iridescence, respectively [Supplementary Material S2]. The samples annealed at  $450$  and  $600^{\circ}\text{C}$  were found to be X-ray-amorphous.

$\text{Yb}^{3+}$  is known as an effective sensitizer to perform upconversion luminescence for  $\text{Er}^{3+}$  [10,11]. Upconversion in materials doped with  $\text{Er}^{3+}$  and  $\text{Yb}^{3+}$  ions occurs due to energy transfer between the lanthanide ions and is effective for the excitation wavelength of 980 nm due to the large absorption cross-section of ytterbium ions [10–12]. We may assume that the dominant mechanism of upconversion luminescence under 980 nm excitation for the  $\text{BaTiO}_3:(\text{Er},\text{Yb})$  xerogel in the opal matrix and onto the surface of the opal matrix is the absorption by  $\text{Yb}$  ions and the energy transfer from  $\text{Yb}^{3+}$  to  $\text{Er}^{3+}$  [12]. As a result, the luminescence bands corresponding to the transitions from the excited states  $^2\text{H}_{11/2}$ ,

$^4S_{3/2}$ ,  $^4F_{9/2}$ ,  $^4I_{9/2}$  to the ground state  $^4I_{15/2}$  of trivalent Er ions are observed from PL spectra (Figure 5a), and upconversion luminescence is recorded by the camera (Figure 4). Schematic partial energy-level diagrams for the  $Er^{3+}$ – $Yb^{3+}$  couple demonstrating energy transfer between the lanthanide ions is given in Figure 5b.

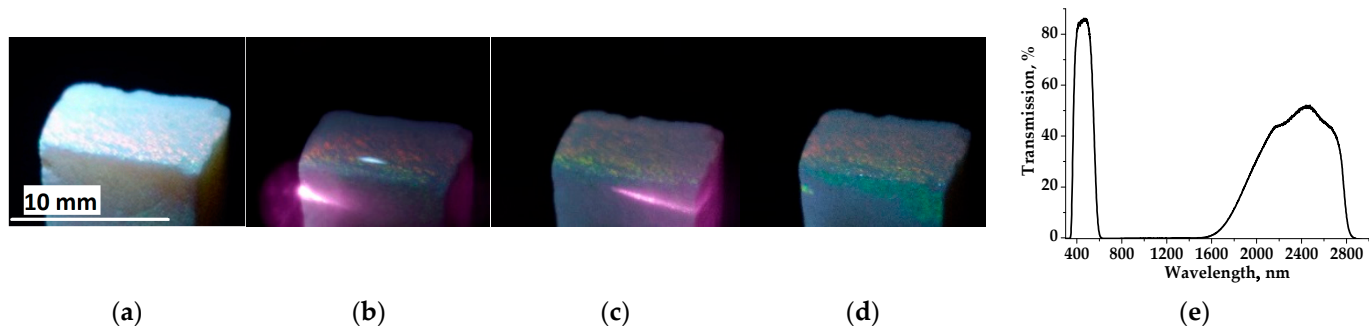


**Figure 4.** Images of opal matrix (sample #4): (a)—without illumination with an IR laser; (b–d)—under illumination with a 980 nm laser. All images are taken from the same sample. The size of the sample is about  $10 \times 9 \times 4$  mm. The sample was mounted vertically on a holder and was poured with ethanol on top to increase iridescence. The orchid color on figures (b,c) is supposed to be the registration by camera of the scattered IR light of the laser scattered by the opal; (d)—the filter with transmission shown in figure (e) is placed between the nearest vertical plane of the opal and the camera; thus, the orchid color is cut. The laser in figure (d) is focused at the left edge, exciting green upconversion luminescence, which is detected by the camera after passing through the filter; (e)—transmission spectrum of the filter.

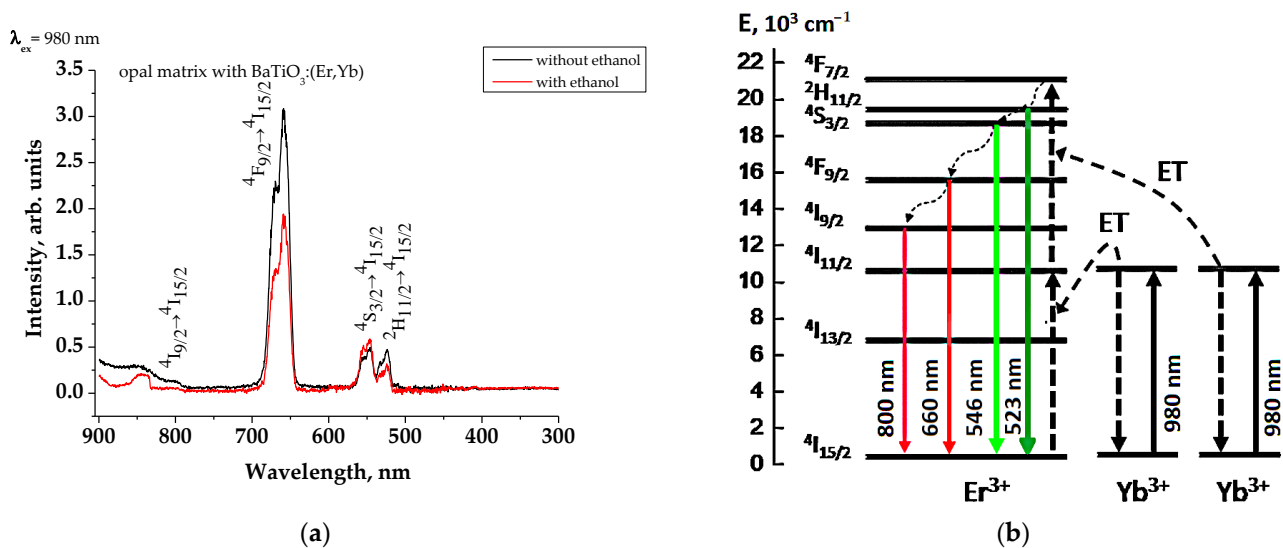


**Figure 5.** Upconversion PL spectra of opal matrix (sample #4) under CW excitation with 980 nm laser (a): 1—dry opal matrix (without ethanol), 2—opal matrix impregnated with ethanol. Schematic partial energy-level diagrams for the  $Er^{3+}$ – $Yb^{3+}$  couple demonstrating energy transfer between the lanthanide ions and the optical transitions corresponding to the upconversion PL bands (b). The wavy arrows indicate nonradiative transitions.

It is worth noting that the camera also records scattered light of the 980 nm laser, adding orchid color to the image. Thus, the penetration path of the scattered light in the xerogel/opal structure also contributes to the individuality of the color image, and this depends on the defects in the opal matrix and the distribution of the xerogel in mesoscopic pores of the opal matrix. In more detail, the scattering of laser radiation in the opal/xerogel structure will also depend on the type of xerogel and its refractive index, i.e., by changing the composition of the sol and the heat treatment temperature, it is possible to obtain new

color images with iridescence effects and registration of scattered laser radiation. Examples of these images are given in Figure 6.



**Figure 6.** Images of opal matrix (sample #4) under illumination with an IR laser. The area illuminated by the laser does not show upconversion luminescence. The orchid color is the scattered light of the laser detected by the camera. The images from (a) to (d) differ in the area of laser illumination and the white light source.

Unlike samples #1 and #2, samples #3 and #4 have lower transmission. The decrease in transmission is due to both an increase in diffuse light scattering after the introduction of xerogel into the pores and partial sintering of the opal matrices during heat treatment. Nevertheless, opal matrices such as samples #3 and #4 retain their mesoporous structure, clusters with regular packing of the globules, photonic stop-band, and iridescence. For example, impregnation of sample #4 with ethanol leads to a red shift in the photonic band gap by 33 nm and an increase in its iridescence (Figure 7).

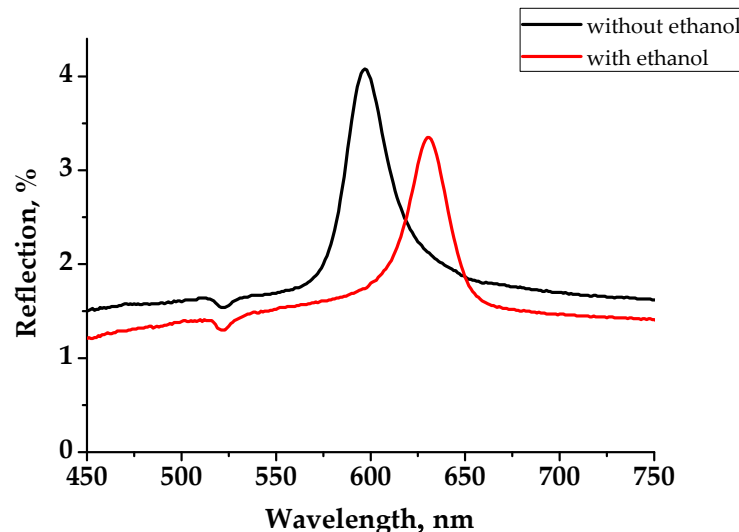


**Figure 7.** Reflection spectra of opal matrix with  $\text{BaTiO}_3:(\text{Er},\text{Yb})$  xerogel: black curve—without ethanol, red curve—with ethanol.

Significantly, controlled, short-term heat treatment at  $600\text{ }^\circ\text{C}$  allows for the observation of both iridescence and upconversion luminescence simultaneously. Thus, from our point of view, application of sol-gel synthesis in opal matrices is an intriguing method of producing color images for show effects. Without a doubt, inverted opal structures made of titania, vanadium oxide, barium titanate, and other materials [13–16], as well as opal matrices with liquid crystals [17] and photonic crystals with polarization-dependent reflectivity anisotropy [18], can also be used to create show effects using iridescence and luminescence simultaneously.

#### 4. Conclusions

In conclusion, we report that inexpensive opal matrices allow beautiful multicolor images to be obtained using a very simple experimental setup. The iridescence of the initially opaque opal matrices is enhanced by impregnating them in ethanol, which makes

the matrices more transparent by reducing diffuse scattering. The simultaneous recording of iridescence and scattered laser radiation enhances the visual appeal of opal matrix images when they are illuminated by a laser. The synthesis of xerogel in the mesoporous space between the globules of the opal matrix, in turn, makes the image of scattered laser radiation unpredictable and attractive. Finally, upconversion luminescence of trivalent erbium ions from the xerogel/opal structure adds additional color to the palette of the iridescent sample. Heat treatment at 600 °C for 30 min of BaTiO<sub>3</sub>:(Er,Yb) xerogel/opal matrix allows for observation of iridescence and upconversion luminescence simultaneously. Opal matrix images as a video or slide show can be accompanied by music or vice versa. An example of a video is provided in Supplementary Materials S3, Video S2. Images of opal matrices that change during impregnation with liquids, when lighting changes, and when luminescence is excited can be used at concerts as footage to denote graphic content and color palette for the screen during the artists' performance.

**Supplementary Materials:** The following supporting information can be downloaded at: <https://www.mdpi.com/article/10.3390/photonics12090908/s1>.

**Author Contributions:** Conceptualization, N.V.G.; methodology, S.M.K.; investigation, data curation T.F.R., E.I.L., U.A.Z., B.Z.S.H., V.D.Z. and Y.V.R.; writing—original draft preparation, N.V.G. and A.V.M.; writing—review and editing, V.A.L.; visualization, E.I.L. and U.A.Z.; supervision, V.A.L. and N.I.K.; project administration, N.V.G. All authors have read and agreed to the published version of the manuscript.

**Funding:** This research was funded by Ministry of Education of the Republic of Belarus: project 1.4 of the Belarusian State Scientific Research Program “Chemical processes, reagents and technologies, bioregulators and bioorgchemstry”, project 2.1.02 of the Belarusian State Scientific Research Program “Convergence 2025”, project 3.5 of the Belarusian State Scientific Research Program “Photonics and Electronics for Innovations”; Belarusian Republic Foundation for Fundamental Research, project T23RNF-147.

**Institutional Review Board Statement:** Not applicable.

**Informed Consent Statement:** Not applicable.

**Data Availability Statement:** The original contributions presented in this study are included in the article/Supplementary Material. Further inquiries can be directed to the corresponding author(s).

**Conflicts of Interest:** The authors declare no conflicts of interest. The funders had no role in the design of the study; in the collection, analyses, or interpretation of data; in the writing of the manuscript; or in the decision to publish the results.

## References

1. Sanders, J.V. Diffraction of light by opals. *Acta Cryst.* **1968**, *A24*, 427–434. [[CrossRef](#)]
2. Astratov, V.N.; Bogomolov, V.N.; Kaplyanskii, A.A.; Prokofiev, A.V.; Samoilovich, L.A.; Samoilovich, S.M.; Vlasov, Y.A. Optical spectroscopy of opal matrices with CdS embedded in its pores: Quantum confinement and photonic band gap effects. *Il Nuovo Cimento D* **1995**, *17*, 1349–1354. [[CrossRef](#)]
3. Bogomolov, V.N.; Gaponenko, S.V.; Germanenko, I.N.; Kapitonov, A.M.; Petrov, E.P.; Gaponenko, N.V.; Prokofiev, A.V.; Ponyavina, A.N.; Silvanovich, N.I.; Samoilovich, S.M. Photonic band gap phenomenon and optical properties of artificial opals. *Phys. Rev. E* **1997**, *55*, 7619–7625. [[CrossRef](#)]
4. Gaponenko, N.V.; Unuchak, D.M.; Mudryi, A.V.; Malyarevich, G.K.; Gusev, O.B.; Stepikhova, M.V.; Krasilnikova, L.V.; Stupak, A.P.; Kleshcheva, S.M.; Samoilovich, M.I.; et al. Modification of erbium photoluminescence excitation spectra for the emission wavelength 1.54 μm in mesoscopic structures. *J. Lumin.* **2006**, *121*, 217–221. [[CrossRef](#)]
5. Lonergan, A.; Hu, C.; O'Dwyer, C. Filling in the gaps: The nature of light transmission through solvent-filled inverse opal photonic crystals. *Phys. Rev. Mater.* **2020**, *4*, 065201. [[CrossRef](#)]
6. Lodahl, P.; van Driel, A.F.; Nikolaev, I.S.; Irman, A.; Overgaag, K.; Vanmaekelbergh, D.; Vos, W.L. Controlling the dynamics of spontaneous emission from quantum dots by photonic crystals. *Nature* **2004**, *430*, 654–657. [[CrossRef](#)] [[PubMed](#)]

7. Su, X.; Sun, X.; Wu, S.; Zhang, S. Manipulating the emission intensity and lifetime of  $\text{NaYF}_4:\text{Yb}^{3+},\text{Er}^{3+}$  simultaneously by embedding it into  $\text{CdS}$  photonic crystals. *Nanoscale* **2017**, *9*, 7666–7673. [\[CrossRef\]](#) [\[PubMed\]](#)
8. Gaponenko, N.V.; Labunov, V.A.; Lashkovskaya, E.I.; Zaitsev, V.A.; Kleshcheva, S.M.; Kargin, N.I. Device for Forming a Color Image on a Plane. Russian Federation Patent No. RU2837366C1, 8 May 2024.
9. Samoilovich, M.I.; Samoilovich, S.M. Method of Preparing Synthetic Material with Noble Opal Structure. Russian Federation Patent No. RU2162456C1, 17 March 2000.
10. Li, H.; Wang, X.; Huang, D.; Chen, G. Recent advances of lanthanide-doped upconversion nanoparticles for biological applications. *Nanotechnology* **2020**, *31*, 072001. [\[CrossRef\]](#) [\[PubMed\]](#)
11. Huang, X.; Han, S.; Huang, W.; Liu, X. Enhancing solar cell efficiency: The search for luminescent materials as spectral converters. *Chem. Soc. Rev.* **2013**, *42*, 173–201. [\[CrossRef\]](#) [\[PubMed\]](#)
12. Lashkovskaya, E.I.; Gaponenko, N.V.; Stepikhova, M.V.; Yablonskiy, A.N.; Andreev, B.A.; Zhivulko, V.D.; Mudryi, A.V.; Martynov, I.L.; Chistyakov, A.A.; Kargin, N.I.; et al. Optical properties and upconversion luminescence of  $\text{BaTiO}_3$  xerogel structures doped with erbium and ytterbium. *Gels* **2022**, *8*, 347. [\[CrossRef\]](#) [\[PubMed\]](#)
13. Wijnhoven, J.E.G.J.; Vos, W.L. Preparation of photonic crystals made of air spheres in titania. *Science* **1998**, *281*, 802–804. [\[CrossRef\]](#) [\[PubMed\]](#)
14. Golubev, V.G.; Davydov, V.Y.; Kartenko, N.F.; Kurdyukov, D.A.; Medvedev, A.V.; Pevtsov, A.B.; Scherbakov, A.V.; Shadrin, E.B. Phase transition-governed opal- $\text{VO}_2$  photonic crystal. *Appl. Phys. Lett.* **2001**, *79*, 2127–2129. [\[CrossRef\]](#)
15. Zhou, J.; Sun, C.Q.; Pita, K.; Lam, Y.L.; Zhou, Y.; Ng, S.L.; Kam, C.H.; Li, L.T.; Gui, Z.L. Thermally tuning of the photonic band gap of  $\text{SiO}_2$  colloid-crystal infilled with ferroelectric  $\text{BaTiO}_3$ . *Appl. Phys. Lett.* **2001**, *78*, 661–663. [\[CrossRef\]](#)
16. Shrike Zhang, Y.; Zhu, C.; Xia, Y. Inverse Opal Scaffolds and Their Biomedical Applications. *Adv. Mater.* **2017**, *29*, 1701115. [\[CrossRef\]](#)
17. Busch, K.; John, S. Liquid-Crystal Photonic-Band-Gap Materials: The Tunable Electromagnetic Vacuum. *Phys. Rev. Lett.* **1999**, *83*, 967–970. [\[CrossRef\]](#)
18. Wu, Y.; Nan, J.; Ren, J.; Meng, Z.; Zhang, S.; Wu, S. Polarization-dependent structural colors in  $\text{ZnS}$  Nanosphere-Based Photonic Crystals for Anticounterfeiting Applications. *ACS Appl. Nano Mater.* **2021**, *5*, 423–429. [\[CrossRef\]](#)

**Disclaimer/Publisher’s Note:** The statements, opinions and data contained in all publications are solely those of the individual author(s) and contributor(s) and not of MDPI and/or the editor(s). MDPI and/or the editor(s) disclaim responsibility for any injury to people or property resulting from any ideas, methods, instructions or products referred to in the content.